SPE 84496

Prediction of Sand Production Rate in Oil and Gas Reservoirs

P.J. van den Hoek, SPE, and M.B. Geilikman, Shell International Exploration and Production B.V.

This paper was prepared for presentation at the SPE Annual Technical Conference and Exhibition held in Denver, Colorado, U.S.A., 5-8 October 2003.

Abstract

Most sand production prediction models to date have the capability to indicate whether initial sand production may take place somewehere during the lifetime of a reservoir. However, these models are unable to predict whether the sand production will be 'problematic' (e.g. in terms of erosion, plugging, well sand-up, separator fill, etc.), in particular for systems that have some tolerance towards sand production.

In order to predict whether sand production will be 'problematic', one needs to be able to estimate sand production volumes and rates as a function of, amongst others, bottom-hole load conditions, drawdown, and time. This paper presents a model for the prediction of sand production volumes and rates for any type of clastic oil or gas reservoir. This work builds on successful previous efforts to predict sand production rate in the Canadian heavy oil sands. The current model is a validation of the previous model and its further generalisation to sandstones of any strength (not just unconsolidated) with any reservoir fluid (not just heavy oil), and involves features such as failure of intact sand, post-failure cavity stabilisation, and non-associated viscoplasticity. The model has been calibrated to laboratory experiments.

1. Introduction

Geilikman and coworkers [1-3] developed a simple analytical model to predict the (transient) sand production rate following production start-up or bean-up of wells producing from Canadian heavy oil sands. The essential feature distinguishing this model from conventional elasto-plastic approaches of 'tensile' cavity failure (e.g. [4-5]) is the ansatz that in the presence of fluid flow, the growth of a plastic zone is always associated with a non-zero sand production rate q_s. Thus, upon start-up or bean-up of a well, the boundary between the plastic and elastic zones will grow to a new equilibrium value. As a result of the viscosity of the production fluid and the rock, this boundary growth will not be 'infinitely' fast, but rather take place within a finite timeframe. During this period of plastic zone boundary growth, sand is produced. Note that this type of sand production is entirely different than the one associated with 'tensile' failure at the cavity wall [4,5]. The latter type is more of a catastrophic nature and takes place long after the plastic zone has been formed, whereas the q_s of Geilikman's model is the result of plastic zone extension and is generally of a transient nature.

Further key features of Geilikman's model can be summarised as follows:

- Elastic-perfectly plastic constitutive behaviour
- Weakly consolidated sand without post-failure stabilisation
- Associated visco-plasticity
- Drainage radius much larger than plastic zone radius

The results of this model were able to reproduce the field-observed sand production trends in the Canadian heavy oil sands quite well [1-3].

2. Model formulation

The sand production rate model presented here is a generalisation of Geilikman's model to sandstones of any strength (not just unconsolidated) with any reservoir fluid (not just heavy oil). The extensions to Geilikman's model are primarily based on the combined 'compressive'/'tensile' failure sand production prediction model of Refs. [6-7]. Key features of the current model can be summarised as follows:

- Elastic-perfectly plastic constitutive behaviour with a drop in cohesion at the elastic-plastic boundary to represent the impact of intact rock failure.
- Sandstone of any strength (i.e. not just weakly consolidated)
- Post-failure stabilisation – i.e. the cavity strength increases with cumulative amount of produced sand.
- Non-associated visco-plasticity
- Drainage radius needs not be much larger than plastic zone radius. Although in the field, the drainage radius will always be much larger than the plastic zone radius, this is not necessarily true in the laboratory. Therefore, this feature will be particularly useful for analysing laboratory sand production tests.

Mathematical details of the model can be found in Appendix A.

3. Results and discussion

Results (trends) as obtained using this model are presented in the paragraphs below.

Comparison with field data. Figs. 1 and **2** show typical field examples of sand production from a Canadian heavy oil sand. Initially, the sand cut can be very high (order 50%), but with time it drops to 'low' percentages (order 5%, **Fig. 1**) or even disappears altogether (**Fig. 2**). Since the flow velocities are, owing to the high viscosity of the crude, very low, erosion is not really an issue, even not at these high sand cuts.

Fig. 3 shows a match of the results of **Fig. 1** using our model. Input data (**Table 1**) are 'typical' Canadian heavy oil sand data [2]. In fact, for these type of data (very weakly consolidated rock everwhere) our model is essentially similar to Geilikman's model [1-3]. A formation (viscoplastic) viscosity η of 10^{11} Pa.s has been assumed. This is based on data from Refs. [8,9]. However, it should be pointed out that literature data show a large variation, and therefore more work will be required to come up with a realistic estimate of this parameter for oily sands.

As can be seen, **Fig. 3** shows a good match of the field data (at least at a qualitative level). As it turns out, for the Canadian heavy oil sands, the computed trend of sand production rate versus time is fairly insensitive to the exact value of the formation viscosity η. This is mainly due to the fact that the formation fluids are very viscous by themselves. This has led Geilikman to drop the use of this parameter in later versions of his model [2]. For formations producing light crude or gas, however, a viscosity parameter describing the 'retarded' reaction of the formation to external loading is required as otherwise the computed sand production is always characterised by extremely short bursts with very high sand cut, which is not in line with field data.

As a last remark, we want to point out that all sand production of **Figs. 1**–**3** is characterized by the absence of post-failure cavity stabilisation by whatever means (as is to be expected in very weak sandstone, see Ref. [4]). Therefore, the only mechanism responsible for the sand production rate decline as seen in these figures is the fact that the near-wellbore plastic zone has a higher permeability than the 'intact' zone, thus reducing the drawdown-induced drag forces.

Sand production rate as a function of external load and drawdown. Figure 4 shows results for transient sand production after opening up the well in a reservoir with 'Castlegate sandstone' properties (TWC = 400 bar) and with 'Salt Wash South' sandstone properties (TWC = 200 bar) (see **Table 2** for input parameters, which are based on laboratory tests). The figure shows the cumulative amount of produced sand, and the sand production period (= the time it takes for the sand production rate to decline to zero), as a function of the near-wellbore vertical effective stress. As is clear from **Fig. 4**, both the produced sand volume and the sand production period strongly depend on external load and rock strength. These trends appear to be in line with what is generally observed in the laboratory and in the field.

Figure 5 also shows results for transient sand production after opening up the well, but in this case the sand volumes and transient periods are plotted as a function of final applied drawdown (normalised over the $UCS^{(p)}$ of the failed zone). As can be seen, these parameters also depend on drawdown, in line with expectations. However, the dependency is much weaker than on far-field stress (compare **Fig. 4**). The only strong relative increase of sand volume with increasing drawdown can be seen in the area where the drawdown is of the same order as $UCS^{(p)}$. For higher drawdowns, the failed rock is largely transported into the wellbore and the cumulative sand volume hardly increases anymore with increasing drawdown.

Sand production rate as a function of failed zone strength **Figures 6** and **7** show the cumulative sand volumes and sand production periods of transient sand production as a function of failed zone strength. As can be seen, there is a clear dependency of sand volume and production period on the strength of the failed zone, especially for higher loads and/or weaker materials, which is in line with expectations. Note that for very weak failed rock and high loading, sand will be produced forever.

From **Figs. 6** and **7**, it is clear that the impact of watercut, which will tend to lower the strength of the failed zone, is properly captured within the sand production model, at least at a qualitative level.

Comparison with Bratli / Risnes 'tensile' failure criterion. According to the well-known Bratli-Risnes criterion, applying a drawdown beyond a specified 'tensile failure' limit leads to cavity collapse and subsequent massive sand production [4,5]. Within the framework of the current model, this criterion can be related to a drawdown limit above which the sand production rate q_s no longer declines to zero but instead reaches a minimum value and subsequently increases again. This only applies to very weakly consolidated sandstones that do not exhibit any post-failure cavity stabilisation.

Figures 8 and **9** show the sand cut and corresponding normalised pressure gradient g_{pn} as a function of time and of the strength of the failed rock. The relevance of the quantity g_{pn} is found in the Bratli-Risnes criterion, which states that for cylindrical cavities, tensile failure takes place if $g_{pn} \geq UCS^{(p)}$, where $UCS^{(p)}$ is the unconfined compressive strength of the failed zone. The normalised pressure gradient g_{pn} is directly proportional to the applied drawdown.

As can be seen from **Figs. 8** and **9**, for low enough drawdown (or, conversely, high enough failed rock strength), the sand production rate declines to zero, but for higher drawdowns (lower failed rock strength), the sand cut does not decline to zero but instead reaches a minimum and subsequently starts to increase again. This happens already for drawdowns (i.e. normalised pressure gradients) below the Bratli-Risnes limit, as can be seen by comparing **Figs. 8** and **9**. A precise criterion for determining whether the sand cut will decline or whether it will eventually blow up is provided in Appendix A.

The above results provide an interpretation of how the Bratli-Risnes criterion translates to field conditions. It is, however, important to bear in mind that these results only apply to those sandstones where post-failure cavity stabilisation does not occur, i.e. only to very weakly consolidated, non-dilatant sandstones [10].

4. Conclusions

The results of this work can be summarised as follows:

- Sand production trends and volumes as predicted by the model are able to reproduce field observed sand production trends and volumes.
- Sand production rate, volume, and time (for transient sand production) show a significant increase with increasing load and drawdown once the load has exceeded the limit for initial failure; this is in line with field observations.
- Sand rate, volume and time also significantly increase with decreasing 'effective' cohesion of the failed sand pack immediately surrounding the wellbore; this phenomenon helps to explain the general observation that watercut leads to enhanced sand production.
- If the intact formation sandstone is only weakly consolidated and non-dilatant, it can be shown that for a sufficiently high drawdown (which is related to the well-known Bratli-Risnes criterion), the sand production rate can initially stabilise (exhibiting itself as an 'apparent' transient sand production), but at a later stage it can 'explode' until eventually the well sands up.

Nomenclature

F	Yield function
φ	Friction angle
ϕ_i	Porosity of intact zone
ϕ_p	Porosity of plastic zone
G	Plastic potential
g_{pn}	$\equiv -r*\partial\Delta P/\partial t$ Normalised drawdown gradient
γ_p	Poro-elastic (depletion / inflation) constant
k_i	Permeability of intact zone
k_p	Permeability of plastic zone
μ	Oil viscosity
η	Visco-plastic viscosity of sand
p_e	Reservoir pressure at drainage radius
p_c	Critical wellbore pressure at which formation of yielded zone starts
p_∞	Wellbore pressure at $t=\infty$
ψ	Dilatancy angle
Q_f	Fluid flow rate per metre of hole
q_s	Sand production rate per metre of hole
r_w	Wellbore radius
r_e	Drainage radius
R	Radius of plastic zone
S	Cumulative amount of produced sand per metre of hole
S_p	Constant charactersing the total volume of sand produced prior to full PFS
σ_r	Radial effective stress
σ_ϑ	Tangential effective stress
σ_∞	Far-field effective stress
σ_i	Radial effective stress at borehole wall
t	Time
t_p	Constant characterising the speed of wellbore pressure reduction
T	$= 2\sin\varphi/(1-\sin\varphi)$
$UCS^{(e)}$	UCS of intact zone
$UCS^{(p)}$	UCS of plastic zone
v_s	Sand production velocity

Acknowledgment

The authors are grateful to Shell Internationale Exploration and Production B.V. for permission to publish this work.

References

1. M.B. Geilikman, M.B. Dusseault, and F.A.L. Dullien. Sand production as a viscoplastic granular flow. SPE 27343 (1994).
2. M.B. Geilikman, and M.B. Dusseault. Fluid rate enhancement from massive sand production in heavy-oil reservoirs. J. Pet. Science Eng. 17 (1997) 5-18.
3. M.B. Geilikman, M.B. Dusseault, and F.A.L. Dullien. Fluid production enhancement by exploiting sand production. SPE 27797 (1994).
4. Bratli, R.K. and Risnes, R., 1981, "Stability and failure of sand arches", SPE Journal, April 1981, pp. 236-248.
5. Risnes, R., Bratli, R.K. and Horsrud, P.: "Sand stresses around a wellbore," SPE Journal (Dec. 1982) 883-898.
6. P.J. van den Hoek, GH.M.M. Hertogh, A.P. Kooijman, P. de Bree, C.J. Kenter and E. Papamichos. A new concept of sand production prediction: theory and laboratory concepts. SPE Drilling & Completions Journal, December 2000, 261-273
7. P.J. van den Hoek, A.P. Kooijman, P. de Bree, C.J. Kenter, Z. Zheng and M. Khodaverdian. Horizontal wellbore stability and sand production in weakly consolidated sandstones. SPE Drilling & Completions Journal, December 2000, 274-283
8. Vyalov, S.S. "Rheological fundamentals of soil mechanics". Developments in Geotechnical Engineering, 36. Elsevier, Amsterdam, 1986. Chapter 4.
9. Katona, M.G. "Evaluation of viscoplastic cap model". J. Geotech. Eng. of ASCE, No. 8 (1984), 1106-1125.
10. P.J. van den Hoek. Prediction of different types of cavity failure using bifurcation theory. 38th US Rock Mechanics Symposium, Washington DC, USA, 7-10 July 2001.

APPENDIX A. Analytical expressions for sand production rate from cylindrical cavities

In this Appendix, analytical expressions are derived for sand production rate from cylindrical cavities. The expressions are an extension to Geilikman's model [1-3]. The latter was developed for unconsolidated sandstones using an elastic-perfectly plastic model. This model used certain approximations which are only valid if the drainage radius is much larger than the radius of the plastic zone.

In this Appendix, an exact expression for sand production rate is derived for any ratio of drainage radius to plastic zone radius. This expression is exended to the case of sandstones with cohesion, and to the case of stabilising hole (post-failure stabilisation) and non-associated viscoplasticity.

The equations in this Appendix are to a large extent based on the expressions of [1,7].

A.1 Basic formulation

Consider a cylindrical cavity with inner-hole radius r_w, plastic radius R and drainage radius r_e. Fluid flow (flow rate per metre of hole Q_f) is flowing into the cavity. At the same time, sand production (rate per metre of hole q_s) from the cavity

wall takes place (provided the sand is plastic there). Since the porosity ϕ_p of the sand in the plastic zone is larger than the porosity ϕ_I , this sand production can be associated with a growth of the plastic zone. As soon as the fluid flow is switched on, sand production will cause the plastic zone to grow until it has reached its equilibrium value for that particular flow rate.

Within this formulation, the plastic radius is related to sand production as [1]

$$R(t)=\sqrt{r_w^2+\frac{S(t)}{\pi(\phi_p-\phi_i)}} \qquad \text{(A1a)}$$

where S is the cumulative amount of sand produced per metre of hole, i.e. we have

$$q_s(t)=\frac{dS}{dt} \qquad \text{(A1b)}$$

The pressure drops Δp_p and Δp_i over the plastic and intact (elastic) zones, respectively, are given by [1]

$$\Delta p_p=\frac{\mu}{2\pi k_p}\left(\frac{Q_f}{\phi_p}-\frac{q_s}{1-\phi_p}\right)\ln\left(\frac{R}{r_w}\right) \qquad \text{(A2a)}$$

$$\Delta p_i=\frac{\mu}{2\pi\phi_i k_i}Q_f\ln\left(\frac{r_e}{R}\right) \qquad \text{(A2b)}$$

The total pressure drop Δp_e is given by the combined pressure drops over plastic and intact zones:

$$\Delta p_e=p_e-p_w=\Delta p_p+\Delta p_i \qquad \text{(A3)}$$

Now, when switching the flow on, we assume that the total pressure drop Δp_e remains constant over time [1].

We can now express the fluid flow rate Q_f in terms of the sand rate q_s by combining Eqs. (A1)-(A3) and re-arranging:

$$Q_f(t)=\frac{p_e-p_w+\frac{\mu}{2\pi k_p\phi_p}\frac{q_s(t)}{1-\phi_p}\ln\left(\frac{R(t)}{r_w}\right)}{\frac{\mu}{2\pi}\left(\frac{\ln(R(t)/r_w)}{k_p\phi_p}+\frac{\ln(r_e/R(t))}{k_i\phi_i}\right)} \qquad \text{(A4)}$$

where μ is the viscosity of the flowing fluid, and k_p and k_i are the permeabilities of the plastic and intact zones, respectively.

The next step is to express the radial stresses in terms of the sand flow rate q_s. From Ref. [7], we have for the radial stress $\sigma_r(R)$ at the plastic-intact interface,

$$\sigma_r(R)=\frac{UCS^{(p)}+T\sigma_i-g_{pn}^p}{T}\left\{\left(\frac{R}{r_w}\right)^T-1\right\}+\sigma_i \qquad \text{(A5)}$$

where $UCS^{(p)}$ is the cohesion-based UCS in the plastic zone [7], the quantity T is given by

$$T=\frac{2\sin\varphi}{1-\sin\varphi} \qquad \text{(A6)}$$

(with φ the friction angle), σ_i is the cavity support stress and the quantity g_{pn}^p is the normalised pore pressure gradient of the plastic zone, given by

$$g_{pn}^p=\frac{\mu}{2\pi k_p\phi_p}\left(Q_f-\frac{q_s}{1-\phi_p}\right) \qquad \text{(A7)}$$

(note that the analogous normalised pore pressure gradient for the intact zone g_{pn}^i is given by

$$g_{pn}^i=\frac{\mu}{2\pi k_i}\frac{Q_f}{\phi_i} \qquad \text{(A8)}$$

The radial stress at infinity σ_∞, is also given in [7],

$$\sigma_\infty=\sigma_r(R)-\left(1-\tfrac{1}{2}\gamma_p\right)g_{pn}^i\ln\left(\frac{r_e}{R}\right)+\tfrac{1}{2}UCS^{(e)}+\tfrac{1}{2}T\sigma_r(R)-\tfrac{1}{4}\gamma_p g_{pn}^i$$

(A9)

where $UCS^{(e)}$ is the cohesion-based UCS in the intact (elastic) zone, and $\sigma_r(R)$ is given by Eq. (A5).

Combining Eqs. (A4)-(A9) allows us to write an expression for the sand rate q_s in the following form:

$$q_s=\frac{E-\sigma_\infty}{F} \qquad \text{(A10a)}$$

with

$$E=\frac{UCS^{(p)}+T\sigma_i-\frac{\mu}{2\pi k_p}\frac{A}{\phi_p}\left(1+\frac{1}{2}T\right)\left\{\left(\frac{R}{r_w}\right)-1\right\}}{T}$$

$$-\frac{\mu}{2\pi k_i}\frac{A}{\phi_i}\left\{\left(1-\frac{1}{2}\gamma_p\right)\ln\left(\frac{r_e}{R}\right)+\frac{1}{4}\gamma_p\right\}+\frac{1}{2}UCS^{(e)} \qquad \text{(A10b)}$$

$$F=\frac{\mu D}{2\pi k_p T}\left(1+\frac{1}{2}T\right)\left\{\left(\frac{R}{r_w}\right)-1\right\}+\frac{\mu}{2\pi k_i}\frac{B}{\phi_i}\left\{\left(1-\frac{1}{2}\gamma_p\right)\ln\left(\frac{r_e}{R}\right)+\frac{1}{4}\gamma_p\right\}$$

(A10c)

$$A=\frac{p_e-p_w}{\frac{\mu}{2\pi}\left(\frac{\ln(R/r_w)}{k_p\phi_p}+\frac{\ln(r_e/R)}{k_i\phi_i}\right)} \qquad \text{(A10d)}$$

$$B=\frac{\frac{\mu}{2\pi k_p\phi_p}\frac{\ln(R/r_w)}{1-\phi_p}}{\frac{\mu}{2\pi}\left(\frac{\ln(R/r_w)}{k_p\phi_p}+\frac{\ln(r_e/R)}{k_i\phi_i}\right)} \qquad \text{(A10e)}$$

$$D = \frac{1}{\phi_p}\left(B - \frac{1}{1-\phi_p} \right) \tag{A10f}$$

Combination of Eqs. (A1) and (A10) yields a differential equation in R(t) which can be integrated in time, from which the sand rate $q_s(t)$ follows.

A.2 Initial condition: sand rate for R=r_w

In line with [1], upon opening up production, the bottomhole pressure at the wellbore is assumed to drop exponentially from a value p_c at which the sandstone at r_w just starts to yield, to a value p_∞ which is the stabilised bottom-hole pressure at t=∞:

$$p(t) = p_\infty + (p_c - p_\infty)e^{-t/t_p} \tag{A11}$$

where t_p is a constant characterising the speed of pressure reduction. We now can calculate p_c from the requirement that for $p_w=p_c$ and $R=r_w$, we must have $\sigma_\infty=E$ (E given by Eq. (A10b)). This requirement follows from the fact that the coefficient F given by (A10c) is equal to zero for $R=r_w$ and q_s for $R=r_w$ must be a finite number (see Eq. (A10a)). Substituting the above requirement in the relevant equations yields

$$p_c = p_e - \frac{\frac{1}{2}UCS^{(e)} + \left(\frac{1}{2}T + 1\right)\sigma_i - \sigma_\infty}{1 - \frac{1}{2}\gamma_p + \frac{1}{4}\gamma_p \Big/ \ln\left(\frac{r_e}{r_w}\right)} \tag{A12}$$

In order to calculate q_s for $R=r_w$, we have to use Eq. (A10a) in the limit $R\rightarrow r_w$ and $p_w\rightarrow p_c$, where p_w is the wellbore pressure. We write

$$R = r_w(1+\varepsilon) \qquad p_w = p_c(1-\delta) \tag{A13}$$

Substituting this in Eq. (A10a) then yields to first order in δ and ε

$$q_s = \frac{\frac{\delta}{\varepsilon}p_c\left(1 - \frac{1}{2}\gamma_p + \frac{\frac{1}{4}\gamma_p}{\ln(r_e/r_w)}\right) - \left[UCS^{(p)} - \frac{k_i\phi_i}{k_p\phi_p}\frac{p_e - p_w}{\ln(r_e/r_w)}\right]\left(1 + \frac{1}{2}T\right)}{\frac{\mu}{2\pi k_p\phi_p(1-\phi_p)}\left(\frac{1}{2}T + \frac{1}{2}\gamma_p - \frac{\frac{1}{4}\gamma_p}{\ln(r_e/r_w)}\right)} \tag{A14}$$

The increments δ and ε can be further elaborated using

$$R(t+\Delta t) = R(t) + q_s(t)\frac{1}{2\pi R(t)(\phi_p - \phi_i)}\Delta t = R(1+\varepsilon) \tag{A15a}$$

$$p_w(t+\Delta t) = p_w(t) - (p_c - p_\infty)\frac{\Delta t}{t_p} = p_c(1-\delta) \tag{A15b}$$

Substituting Eqs. (A15) for δ and ε into Eq. (A14) finally results in a quadratic equation for the initial sand rate i.e. the sand rate for $R=r_w$:

$$aq_s^2 + bq_s + c = 0 \tag{A16a}$$

$$a = \frac{\mu}{2\pi k_p\phi_p(1-\phi_p)}\frac{T + \gamma_p - \frac{\frac{1}{2}\gamma_p}{\ln(r_e/r_w)}}{2\pi R^2(\phi_p - \phi_i)} \tag{A16b}$$

$$b = \left[UCS^{(p)} - \frac{k_i\phi_i}{k_p\phi_p}\frac{p_e - p_w}{\ln(r_e/r_w)}\right]\frac{1 + \frac{1}{2}T}{2\pi R^2(\phi_p - \phi_i)} \tag{A16c}$$

$$c = -(p_c - p_\infty)\frac{1}{t_p}\left(1 - \frac{1}{2}\gamma_p + \frac{\frac{1}{4}\gamma_p}{\ln(r_e/r_w)}\right) \tag{A16d}$$

A.3 Post failure stabilisation (PFS) of the cavity

PFS is handled by letting $UCS^{(e)}$ increase with the amount of sand produced S:

$$UCS^{(e)}(S) = STAB * UCS^{(e)}(S=0) - (STAB-1) * UCS^{(e)}(S=0)e^{-S/S_p} \tag{A17}$$

where STAB is the maximum cavity stabilisation factor and S_p is a constant characterising the amount of sand produced prior to full PFS of the cavity. These parameters can be calibrated to laboratory or field experiments. All the equations of the previous sections still hold, except that the initial sand rate q_s for $R=r_w$ needs to be modified. Going through the same procedure as the one leading to Eqs. (A16) yields the same result, except that the factor b of (A16c) requires the addition of an extra term, i.e.

$$b \rightarrow b + \frac{1}{2}UCS^{(e)}\frac{STAB - 1}{S_p} \tag{A18}$$

A.4 Visco-plasticity

In the case of a positive Mohr-Coulomb yield function F>0, the relationship in the plastic zone between the tangential stress σ_ϑ and the radial stress σ_r is given by

$$\sigma_\vartheta = UCS^{(p)} + (T+1)\sigma_r + \frac{2}{1-\sin\varphi}F \tag{A19}$$

The stress equilibrium equation now becomes

$$\frac{d\sigma_r}{dr} - \frac{T}{r}\sigma_r = \frac{UCS^{(p)}}{r} - \frac{dP}{dr} + \frac{2}{1-\sin\varphi}\frac{F}{r} \tag{A20}$$

An expression for the yield function F is derived below using the viscoplastic flow rule. The visco-plastic flow is governed by the Hohenemser-Prager-Malvern flow rule [1]. Contrary to [1],

we use the non-associated form of this flow rule, given by

$$\eta\frac{\partial v_s}{\partial r}=-F\frac{\partial G}{\partial \sigma_r}\qquad \eta\frac{v_s}{r}=-F\frac{\partial G}{\partial \sigma_\vartheta}\qquad (F>0)\qquad (A21)$$

where η is the viscoplastic viscosity, $v_s(r)$ is the sand production flow velocity and G is the plastic potential (note: Ref. [1] uses the associated flow rule in this case with G=F),

$$G=\frac{1}{2}(\sigma_\vartheta-\sigma_r)-\frac{1}{2}(\sigma_\vartheta+\sigma_r)\sin\psi+const \qquad (A22)$$

where ψ is the dilatancy angle. Substituting (A22) in (A21) yields

$$\eta\frac{\partial v_s}{\partial r}=F*\frac{1}{2}(1+\sin\psi)\qquad \eta\frac{v_s}{r}=-F*\frac{1}{2}(1-\sin\psi) \qquad (A23)$$

The resulting differential equation for $v_s(r)$ is

$$\frac{\partial v_s}{\partial r}+\frac{1+\sin\psi}{1-\sin\psi}\frac{v_s}{r}=0 \qquad (A24a)$$

with boundary condition

$$v_s(r_w)=\frac{-q_s}{2\pi(1-\phi_p)r_w} \qquad (A24b)$$

The solution is

$$v_s(r)=\frac{-q_s}{2\pi(1-\phi_p)}\frac{r_w^{\frac{2\sin\psi}{1-\sin\varphi}}}{r^{\frac{1+\sin\psi}{1-\sin\psi}}} \qquad (A25)$$

Combining Eqs. (A23) and (A25) now results in an expression for F:

$$F=\frac{q_s}{2\pi(1-\phi_p)}\eta\frac{2}{1-\sin\psi}\frac{r_w^{\frac{2\sin\psi}{1-\sin\varphi}}}{r^{\frac{2}{1-\sin\psi}}} \qquad (A26)$$

Substitution of (A26) into the differential equation (A20) and solving this differential equation according to the methodology of [7] results in the following expression for the radial stress $\sigma_r(R)$ at the plastic-intact interface (compare Eq. (A5)):

$$\sigma_r(R)=\frac{UCS^{(p)}+T\sigma_i-g_{pn}^p}{T}\left\{\left(\frac{R}{r_w}\right)^T-1\right\}+\sigma_i$$

$$+\frac{2}{1-\sin\varphi\sin\psi}\frac{\eta q_s}{2\pi(1-\phi_p)}\frac{1}{r_w^2}\left\{\left(\frac{R}{r_w}\right)^T-\left(\frac{r_w}{R}\right)^{\frac{2}{1-\sin\psi}}\right\} \qquad (A27)$$

Again, by combination of Eqs. (A4)-(A9), but using Eq. (A27) instead of Eq. (A5), results in Eq. (A10) for the sand production rate $q_s(t)$, where now an extra visco-plastic term has to be added to the coeficient F (not to be confused with the yield function) of Eq. (A10c):

$$F\rightarrow F-\left(1+\frac{1}{2}T\right)\frac{2}{1-\sin\varphi\sin\psi}\frac{\eta}{2\pi(1-\phi_p)}\frac{1}{r_w^2}\left\{\left(\frac{R}{r_w}\right)^T-\left(\frac{r_w}{R}\right)^{\frac{2}{1-\sin\psi}}\right\} \qquad (A28)$$

In the limit of $R=r_w$, the same methodology as applied in paragraph **A.2** results in the quadratic equation (A16) for q_s, but with an extra term added to the coefficient a (compare Eq. (A16b)):

$$a\rightarrow a+\frac{1+\frac{1}{2}T}{2\pi R^2(\phi_p-\phi_i)}\frac{2}{1-\sin\varphi\sin\psi}\frac{\eta}{2\pi(1-\phi_p)}\frac{1}{r_w^2}\left(T+\frac{2}{1-\sin\psi}\right) \qquad (A29)$$

A.5 Tensile failure limit

According to the well-known Bratli-Risnes criterion, applying a drawdown beyond a specified 'tensile failure' limit leads to cavity collapse and subsequent massive sand production [4,5]. Within the framework of the current model, this criterion can be related to a drawdown limit above which the sand production rate q_s no longer declines to zero but instead reaches a minimum value and subsequently increases again.

From (A5) and (A9) it follows that in the absence of inner cavity support, the far-field stress is given by

$$\sigma_\infty=\left(UCS^{(p)}-g_{pn}^p\right)\left\{\left(\frac{R}{r_w}\right)^T-1\right\}\left(\frac{1}{T}+\frac{1}{2}\right)-g_{pn}^i\left\{\left(1-\tfrac{1}{2}\gamma_p\right)\ln\left(\frac{r_e}{R}\right)+\tfrac{1}{4}\gamma_p\right\}+\tfrac{1}{2}UCS^{(e)} \qquad (A30)$$

Now, if the sand production rate q_s is to decline to zero, there must be a value for the plastic zone radius R satifying (A30), where the quantities $g_{pn}^{\ p}$ and $g_{pn}^{\ i}$ are given by (compare Eqs. (A7) and (A8))

$$g_{pn}^p=\frac{\mu Q_f}{2\pi k_p\phi_p}\qquad g_{pn}^i=\frac{\mu Q_f}{2\pi k_i\phi_i} \qquad (A31)$$

and Q_f is given by (compare Eq. (A4))

$$Q_f=\frac{p_e-p_w}{\frac{\mu}{2\pi}\left(\frac{\ln(R/r_w)}{k_p\phi_p}+\frac{\ln(r_e/R)}{k_i\phi_i}\right)} \qquad (A32)$$

If no such R can be found, the sand production rate will never decline to zero. As can be seen from the above equations, this will always be the case for drawdowns exceeding the Bratli-Risnes criterion ($g_{pn}^{\ p}=UCS^{(p)}$), but even for drawdowns slightly below this limit Eqs. (A30)-(A32) will have no solution in R. The exact drawdown limit for which there exists no longer a solution will depend on the values of the far-field stress, the constitutive parameters of the rock, plastic zone permeability, etc.

TABLE 1— Sand production parameters Canadian heavy oil sands (example)

TWC(e) = TWC(p)	0.15	(MPa)
sin(phi)	0.25	(-)
mu	5	(Pa.s)
phii	0.32	(-)
ki	1	Darcy
phip	0.4	(-)
kp	2.5	Darcy
re/rw	1000	(-)
gammap	0.6	(-)
pe	3.45	(MPa)
pc	3.0	(MPa)
p(inf)	0.2	(MPa)
tp	1	(day)
sin(psi)	0.25	(-)
Formation viscosity (Eta)	1E+11	(Pa.s)

TABLE 2— Parameters for Castlegate and Salt Wash South

	Castlegate		Salt Wash South	
TWC	40	(MPa)	20	(MPa)
UCS(p)	1	(MPa)	1	(MPa)
sin(phi)	0.5	(-)	0.5	(-)
mu	0.002	(Pa.s)	0.002	(Pa.s)
phii	0.32	(-)	0.32	(-)
ki	1	D	1	D
phip	0.4	(-)	0.4	(-)
kp	2.5	D	2.5	D
re/rw	1000	(-)	1000	(-)
gammap	0.6	(-)	0.6	(-)
pe	15	(MPa)	15	(MPa)
pc	15	(MPa)	15	(MPa)
p(inf)	5	(MPa)	5	MPa)
sigma(inf)	Variable	(Pa)	Variable	(Pa)
tp	800	(sec)	800	(sec)
sin(psi)	0.25	(-)	0.25	(-)
Eta	1E+11	(Pa.s)	1E+11	(Pa.s)

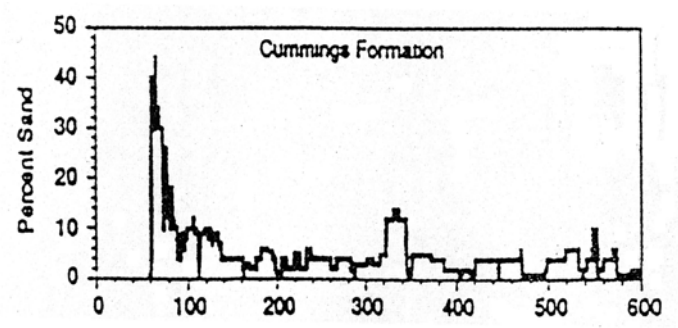

Fig. 1. Typical sand production trend in Canadian heavy oil sands well (Center for Frontier Engineering Research, Edmonton, Alberta).

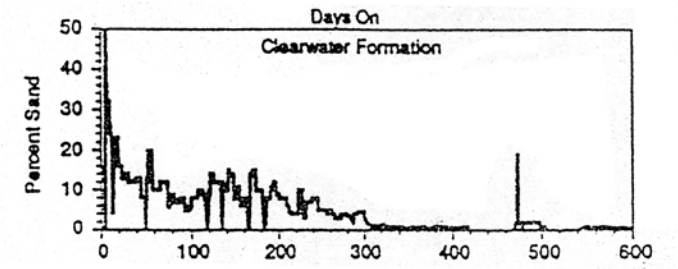

Fig. 2. Typical sand production trend in Canadian heavy oil sands well (Center for Frontier Engineering Research, Edmonton, Alberta).

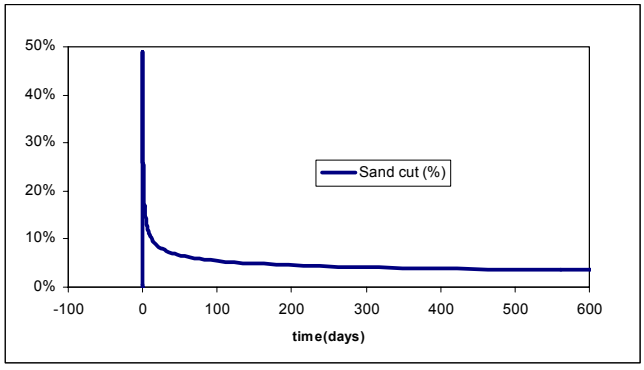

Fig. 3. Match of thr results of Fig. 1. with the analytical sand production model

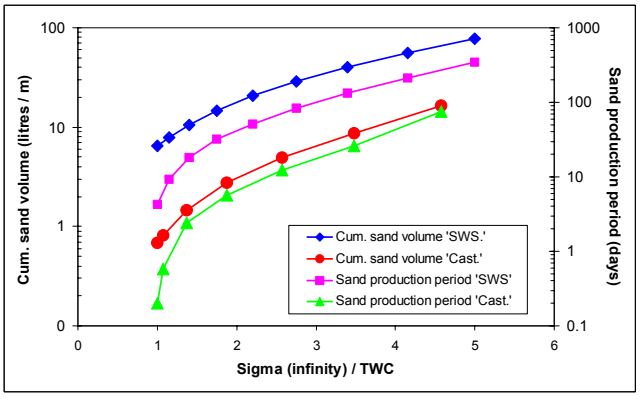

Fig. 4. Computed sand volumes and periods of transient sand production for Castlegate and Salt Wash South sandstones for drawdown/UCS(p) = 1.

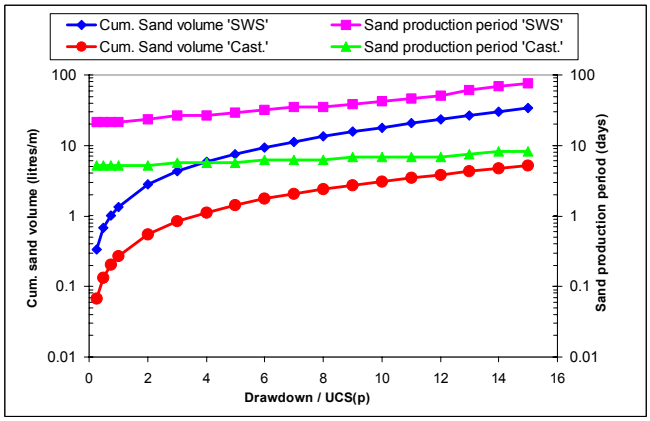

Fig. 5. Computed sand volumes and periods of transient sand production for Castlegate and Salt Wash South sandstones for sigma(inf.)/TWC=2

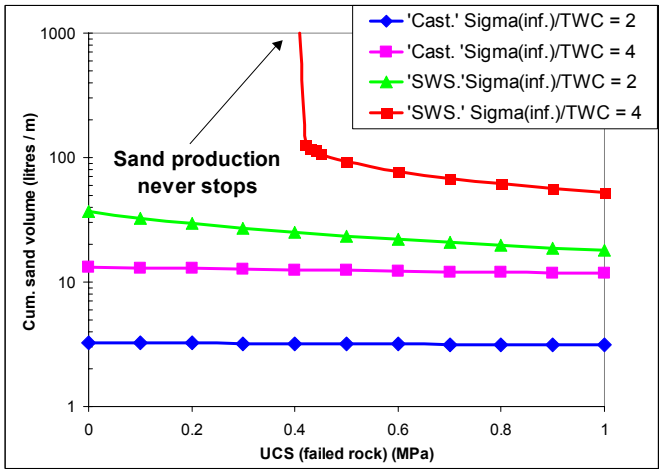

Fig. 6. Computed sand volumes of transient sand production for Castlegate and Salt Wash South sandstones as a function of failed zone strength.

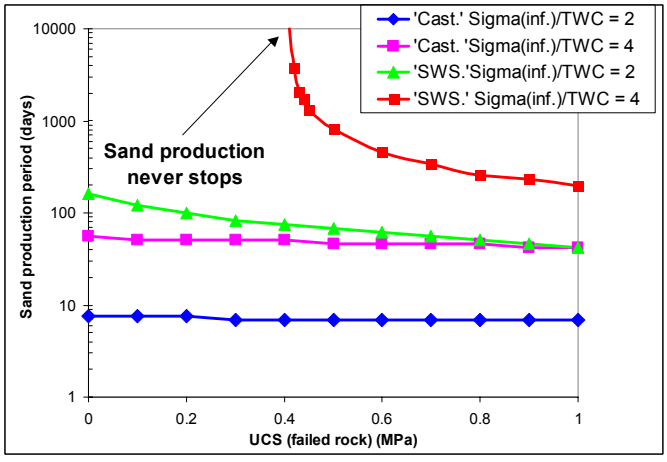

Fig. 7. Computed sand production periods of transient sand production for Castlegate and Salt Wash South sandstones as a function of failed zone strength.

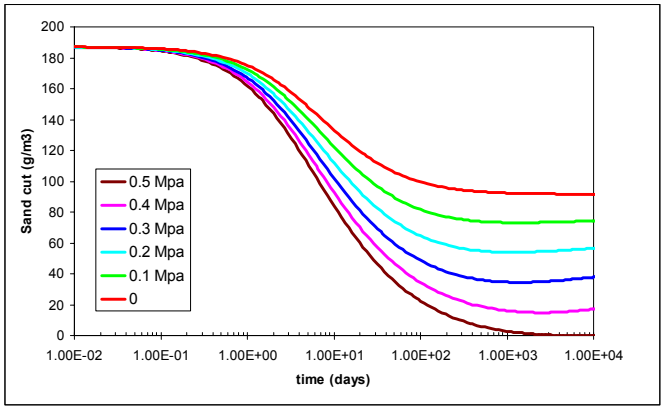

Fig. 8. Computed sand cuts for "SWS-type" sandstone without post-failure cavity stabilisation, as a function of strength of failed rock.

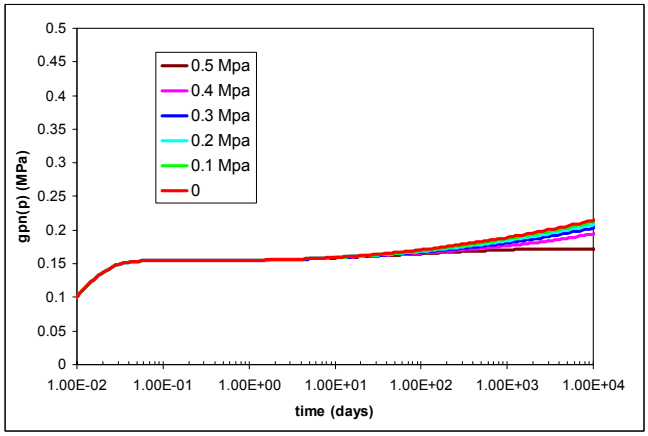

Fig. 9. Computed normalised pressure gradients gpn for "SWS-type" sandstone without post-failure cavity stabilisation, as a function of strength of failed rock.